Comptes Rendus

Physique

Guillaume Cassabois, Adrien Rousseau, Christine Elias, Thomas Pelini, Phuong Vuong, Pierre Valvin and Bernard Gil

Hexagonal boron nitride: optical properties in the deep ultraviolet

CENTRE
MERSENNE

Recent advances in 2D material physics / *Physique des matériaux bidimensionnels*

Hexagonal boron nitride: optical properties in the deep ultraviolet

Nitrure de bore hexagonal : propriétés optiques dans l'ultraviolet profond

Guillaume Cassabois[*], [ORCID] [a], **Adrien Rousseau**[a], **Christine Elias**[a], **Thomas Pelini**[ORCID] [a], **Phuong Vuong**[ORCID] [a], **Pierre Valvin**[ORCID] [a] and **Bernard Gil**[ORCID] [a]

[a] Laboratoire Charles Coulomb, UMR 5221 CNRS-Université de Montpellier, 34095 Montpellier, France

E-mails: guillaume.cassabois@umontpellier.fr (G. Cassabois), adrien.rousseau@umontpellier.fr (A. Rousseau), christine.elias@ens-paris-saclay.fr (C. Elias), thomas.pelini@lncmi.cnrs.fr (T. Pelini), vuongquynhphuong90@gmail.com (P. Vuong), pierre.valvin@umontpellier.fr (P. Valvin), bernard.gil@umontpellier.fr (B. Gil)

Abstract. We review the recent advance in the understanding of the optoelectronic properties of hexagonal boron nitride (hBN) in the deep ultraviolet. The comparison between bulk hBN and monolayer hBN highlights some of their major differences such the bandgap nature, the excitonic binding energy and the phonon-assisted broadening of the excitonic lines. Perspectives point out the relevance of addressing the regime of hBN samples made of a very few number of monolayers, including twisted hBN monolayers in the context of twistronics.

Résumé. Cette revue est dédiée aux progrès récents dans la compréhension des propriétés optoélectroniques du nitrure de bore hexagonal (hBN) dans l'ultraviolet profond. La comparaison entre un cristal massif de hBN et une monocouche de hBN montre quelques unes de leurs différences majeures telles que la nature de la bande interdite, l'énergie de liaison excitonique ainsi que l'élargissement des raies excitoniques assisté par phonons. Les perspectives mettent en avant la nécessité d'étudier le régime d'échantillons composés de quelques monocouches de hBN, y compris des monocouches tournées dans le contexte actuel de la twistronique.

Keywords. hBN, Ultraviolet, Spectroscopy, 2D crystals, Monolayer.

Mots-clés. hBN, Ultraviolet, Spectroscopie, Cristaux 2D, Monocouche.

---

[*] Corresponding author.

1. Introduction

The revolution of 2D materials started with the advent of graphene [1]. Although lamellar materials form a well-characterized class of crystals, the isolation and study of atomically-thin layers have opened a new chapter in the long and rich history of solid state physics. After graphene and its exceptional properties arising from a Dirac cone-energy dispersion, transition metal dichalcogenides (TMDs) have broadened the scope of 2D materials to fascinating optical properties [2]. The indirect–direct crossover of the bandgap at the monolayer limit has been identified as an ubiquitous signature in TMDs. Moreover, the possibility to control the valley degree of freedom in optical pumping experiments has led to the emergence of the new field of valleytronics. Stacking and combining various 2D materials was early recognized as an amazing resource enlarging the study of atomic monolayers to complex van der Waals (vdW) heterostructures [3].

In 2D materials research, hexagonal boron nitride (hBN) is a key compound. With the same honeycomb structure as graphene, hBN further possesses lattice parameters strikingly close to the ones of graphite [4], despite the different nature of the chemical elements forming these crystals and the corresponding huge bandgap variation. With an ultrawide bandgap of ~6 eV [5] hBN is often considered as a sort of ideal insulating 2D material, an excellent substrate for graphene and the best barrier material in vdW heterostructures.

hBN is also emerging as an exciting material in its own right, offering novel material properties that enable a broad range of optical, electro-optical and quantum optics functionalities [6, 7]. The outstanding photonic properties of hBN span very different spectral domains. It is a natural hyperbolic material in the mid-IR range, it hosts defects that can be engineered to obtain room-temperature, single-photon emission in the visible and near-IR range, and it exhibits exceptional properties in the deep-UV for a new generation of emitters and detectors in the UV-C. Interestingly, in contrast to TMDs, both the monolayer and the bulk phases have fascinating opto-electronic properties in the case of hBN.

Here, we present a comparative review of monolayer and bulk hBN, focusing on the recent advance in the understanding of the deep-UV optical response of this 2D material.

2. Monolayer vs bulk hBN

Thanks to its ultrawide bandgap of ~6 eV, hBN is a 2D material where the optical response exhibits intrinsic and extrinsic signatures speading over several eVs. Free exciton recombination occurs above ~5.7 eV (below ~215 nm), extended defects and shallow levels contribute to the emission between ~5 and 5.7 eV (wavelength between ~215 and 250 nm) and deep levels provide potential single photon sources in the near-UV (4.1 eV) and the visible (2–3 eV) spectral domains [6, 7] and also in the near-IR one, as recently demonstrated [8]. Such a spectral decoupling of the various contributions to the optical response allows to separately study the diverse phenomena underlying the rich physics in hBN. As such, hBN appears as a model system for exploring the potentialities offered by 2D materials. The price to pay is the technical difficulties inherent to optical spectroscopy in the deep-UV, often requiring custom design for the optical elements and setups.

In the following, we compare the deep-UV optoelectronic properties of bulk and monolayer hBN in terms of their bandgap nature, excitonic binding energy and phonon-assisted broadening.

2.1. *Bandgap nature*

Similarly to the well-known phenomenology in TMDs, the nature of the bandgap changes at the monolayer limit in hBN. The single-particle bandgap is calculated to be indirect in bulk hBN and
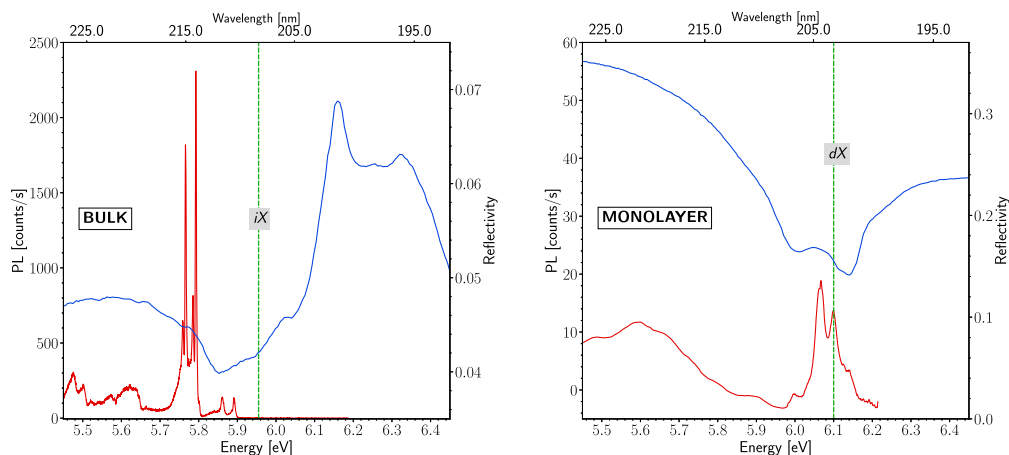
Figure 1. Emission and reflectivity spectra in hBN in the deep ultraviolet, adapted from [10, 11]: (left) bulk hBN, (right) monolayer hBN. The emission (reflectivity) spectra are displayed in red (blue) lines, respectively. The fundamental exciton is indirect in bulk hBN (iX) and direct in monolayer hBN (dX), as indicated by the vertical dashed lines.

direct in monolayer hBN. While the maximum of the valence band sits near the K point of the Brillouin zone in the two cases, the suppression of the interlayer coupling shifts the minimum of the conduction band from the M point in bulk hBN to the K point in monolayer hBN [9].

Such a transition was demonstrated in Ref. [5, 10]. In bulk hBN, the fundamental indirect exciton iX has an energy of ~5.95 eV (Figure 1, left). Because of the indirect bandgap, phonon emission is required during the radiative recombination in order to fulfill momentum conservation. The phonon-assisted emission lines (between 5.7 and 5.9 eV) are thus redshited compared to iX (Figure 1, left) with a detuning given by the energy of the phonon mode involved in the indirect radiative process. From the Stokes shift in emission, one expects an anti-Stokes shift in absorption. Although the absorption spectrum in bulk hBN is to be determined by the interplay between indirect and direct transitions (a open question in the debate initiated by Ref. [12]), we indeed observe in (Figure 1, left) that the reflectivity is blue-shifted compared to iX. The reflectivity peaks around 6.1 eV, in a rather symmetric way compared to the photoluminescence (PL) spectrum. Because of the direct bandgap in the monolayer limit, the results strongly contrast in monolayer hBN (Figure 1, right). The PL and reflectivity spectra have their extrema at the same energy, in resonance with the direct exciton dX, which lies at ~6.1 eV in monolayer hBN.

A major difference between hBN and TMDs is the strong emission in the bulk phase of hBN despite its indirect bandgap. The intense luminescence signal in high-quality hBN crystals was first noted in the pioneering work of Watanabe *et al.* [13]. This striking experimental observation was at the origin of the misinterpretation of the bandgap nature as being direct in bulk hBN. The quantitative estimation of the internal quantum efficiency was recently reported in Ref. [12] with a value as high as 50%, similar to the one of ZnO which is a direct bandgap semiconductor. A possible interpretation for the intense luminescence signal in bulk hBN is the strong exciton–phonon interaction leading to phonon-assisted recombination more efficient than non-radiative recombination. As a consequence of the high radiative efficiency in bulk hBN, the standard strategy followed in TMDs for the demonstration of the bandgap crossover becomes irrelevant in hBN since the simple comparison of the PL signal intensity in monolayer and few-layer (or bulk) hBN is not conclusive. As illustrated by Figure 1, the elucidation of the bandgap nature rather relies on the existence or the absence of a Stokes shift between emission and absorption. From
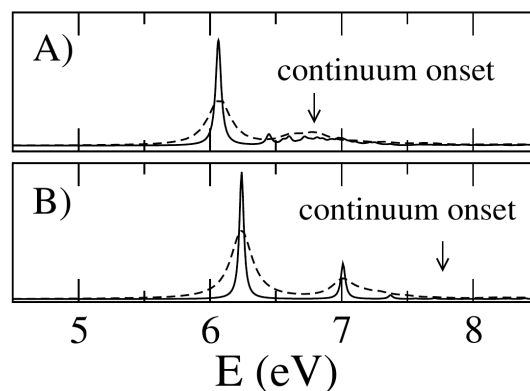
Figure 2. Absorption spectra in hBN: imaginary part of the dielectric permittivity calculated in Ref. [14] for (top) bulk hBN and (bottom) monolayer hBN.

the point of view of applications, the intense emission in bulk hBN makes this semiconductor a promising active material in deep-UV optoelectronic devices, whatever the number of layers.

2.2. *Excitonic binding energy*

Besides the indirect–direct crossover of the bandgap, hBN follows the standard phenomenology of lamellar compounds where the Coulomb interactions are less and less screened when reducing the number of layers. In the monolayer limit, there is a strong increase of the repulsive electron–electron renormalisation and simultaneously of the attractive electron–hole binding. It turns out that the two effects compensate each other [15] (as in carbon nanotubes), so that the direct exciton in monolayer hBN lies approximately at the same energy as the indirect exciton in bulk hBN (Figure 1).

This seemingly constant energy of the bandgap in bulk and monolayer hBN hides the huge enhancement of the excitonic binding energy in monolayer hBN. Because of the screening reduction in the monolayer limit, the binding energy increases from ~0.7 eV in the bulk to ~2 eV in the monolayer hBN, a record value in 2D materials [15]. This huge effect can be directly visualized from the imaginary part of the dielectric permittivity (Figure 2). The vertical arrow in Figure 2 indicates the continuum onset, i.e. the energy of the so-called electronic bandgap corresponding to band-to-band transitions without electron–hole interaction. Because excitons are strongly bound in hBN, the oscillator strength is redistributed towards the excitonic lines, with the fundamental exciton concentrating most of the oscillator strength at the energy of the so-called optical bandgap. The screening reduction in monolayer hBN leads to a blue-shift of the continuum onset to less than ~8 eV (Figure 2), an energy lying in the vacuum-UV spectral domain.

From the point of view of optical spectroscopy, this dramatic increase of the excitonic binding energy induces serious constraints on optical pumping in monolayer hBN. The photo-generation of free electron–hole pair states in the absorption continuum is no longer possible by means of the fourth harmonic of a cw-mode locked Ti:Sa oscillator. While photo-excitation is efficient in bulk hBN at an energy of ~6.3 eV (~196 nm), no PL can be excited at this energy in monolayer hBN. The detection of PL in monolayer hBN requires a selective excitation with a laser detuning matching the energy of one or several phonons [10]. In that case, resonant Raman scattering is superimposed to PL, leading to a distortion of the emission spectrum following the excitation energy [10], as studied in detail on a large range of laser detuning in monolayer MoSe$_2$ [16].
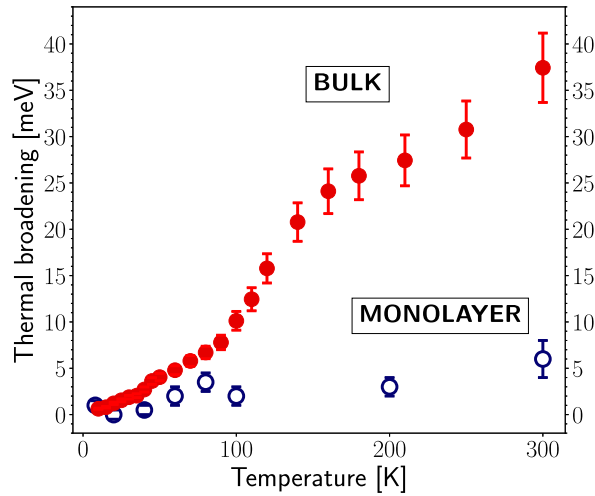
Figure 3. Phonon-assisted broadening in hBN: bulk hBN (full circles) and monolayer hBN (open circles), adapted from Ref. [10, 17]. From 10 K to room temperature, the excitonic linewidth increases by ~35 meV in bulk hBN, in contrast to only ~5 meV in monolayer hBN.

2.3. *Phonon-assisted broadening*

Whereas the previous sections were devoted to a comparison between the electronic properties of bulk and monolayer hBN, we address here their vibrational properties and their impact on the optical response of hBN in the deep-UV. Experimentally, the influence of phonons can be studied from the temperature dependence of the PL spectrum. As far as the thermal redshift of the bandgap energy is concerned, a first indication for the modification of the exciton–phonon interaction is the smaller variation of the bandgap as a function of temperature in monolayer hBN with respect to the bulk phase [10]. A quantitative interpretation of this effect is not straightforward as all phonons contribute to the bandgap shift with temperature [18].

A more direct signature is the phonon-assisted broadening of the excitonic lines which is controlled by a few specific vibrational modes. In bulk hBN, the thermal broadening of the emission lines displays an unusual temperature dependence with a scaling as $\sqrt{T}$ (Figure 3) which comes from the strong coupling of the exciton–phonon broadening [17]. In the bulk phase, the thermal broadening is dominated by the coupling to acoustic phonons below 50 K and to the interlayer breathing mode above 50 K. Interestingly, the isotopic dependence of the thermal broadening could be evidenced in isotopically-purified hBN crystals [18]. In monolayer hBN, the thermal broadening is reduced by a factor ~7 at 300 K in comparison to bulk hBN. Such a modification is due to the suppression of the main broadening process that involves the interlayer breathing mode in bulk hBN, a mode that no longer exists at the monolayer limit. The much weaker temperature dependence of the excitonic linewidth in monolayer hBN (Figure 3) is thus a direct consequence of the reduced number of vibrational modes in a monolayer of 2D material.

3. Towards few-layer hBN crystals

As discussed in this review, bulk and monolayer hBN have different optoelectronic properties that have been investigated by means of complementary experiments in bulk hBN crystals
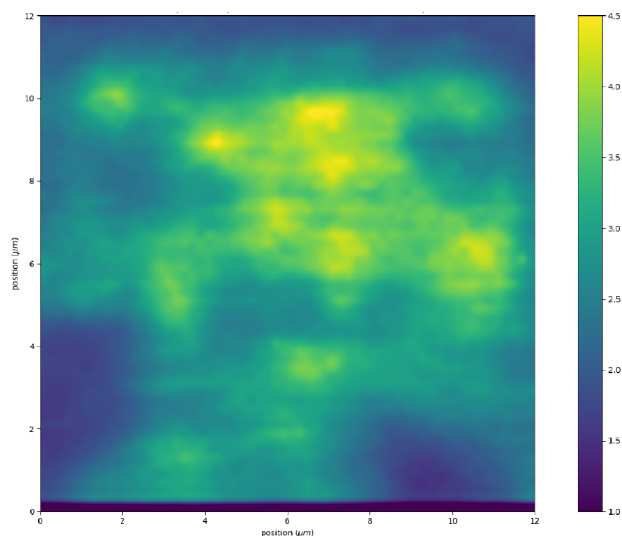
Figure 4. Spatial variations of the PL signal intensity recorded by a deep-UV scanning confocal microscope, in a hBN sample at 8 K, adapted from [11]. The spatial resolution is ~200 nm.

and monolayers of hBN epitaxially grown on graphite. Such a strategy differs from the one usually followed in TMDs which consists in measuring exfoliated few-layer samples with a thickness down to one monolayer. Besides the fact that this strategy is not relevant for physical reasons discussed above and essentially coming from the high internal quantum efficiency in bulk hBN, it has also proven to be of limited use in cathodoluminescence experiments where the emission spectrum could be measured down to only 6 monolayers [19] either because of potential intrinsic limitations of cathodoluminescence for atomically-thin layers of hBN, or because of coupling with the substrate. As a matter of fact, the regime of very few numbers of hBN layers remains unexplored by means of optical spectroscopy in the deep-UV. In this context, the recent achievements in the development of spatially-resolved PL setups in this spectral domain are full of promises [11, 20, 21]. One example is shown in Figure 4 (corresponding to Ref. [11]) where the spatial resolution is of order of ~200 nm in the deep-UV micro-PL experiments for hBN samples at 8 K. The spatial variations of the PL signal intensity around 5.8 eV observed in Figure 4 reveal inhomogeneities of the intrinsic recombination signal. Such a spatial distribution differs from the homogeneous one reported by cathodoluminescence measurements in thin hBN samples exfoliated from crystals synthesized at NIMS-Tsukuba [12], indicating that the relaxation dynamics may display distinct phenomenologies in hBN crystals synthesized by various growth methods.

There has been some detailed characterization of few-layer hBN samples in the last few years. The vibrational properties have been studied by Raman spectroscopy with the evidence for the softening of the low-frequency interlayer shear mode when reducing the number of layers [22]. The valence band-structure was investigated by nano-ARPES experiments with an emphasis on the stacking order differing from the standard AA' one in three- and four-monolayer samples [23]. The issue of the stacking order was studied in the bulk phase [24–26] but the interest in this topic is renewed in few-layer hBN. High-resolution TEM measurements [27] have further pointed out the importance of this aspect and its dependence on the sample preparation procedure, not only in the "top-down" context of exfoliating a bulk hBN crystal but also in the "bottom-up" approach of epitaxy. Finally, we would like to highlight the growing interest in playing with an

additional degree of freedom, i.e. the relative orientation of different monolayers. Magic-angle twisted bilayer graphene has opened perspectives for studying superconductivity arising from electronic interactions, correlated insulator states, spontaneous ferromagnetism and quantum Hall effect. This new field of twistronics has not been experimentally investigated in hBN yet, although theoretical calculations predict fascinating novel properties to be explored in this 2D material with amazing potentialities [28–30].

Acknowledgements

References

[1] K. S. Novoselov, A. K. Geim, S. V. Morozov, D. Jiang, Y. Zhang, S. V. Dubonos, I. V. Grigorieva, A. A. Firsov, "Electric field effect in atomically thin carbon films", *Science* **306** (2004), no. 5696, p. 666-669.

[2] G. Wang, A. Chernikov, M. M. Glazov, T. F. Heinz, X. Marie, T. Amand, B. Urbaszek, "Colloquium: excitons in atomically thin transition metal dichalcogenides", *Rev. Mod. Phys.* **90** (2018), no. 2, article no. 021001.

[3] A. K. Geim, I. V. Grigorieva, "Van der Waals heterostructures", *Nature* **499** (2013), no. 7459, p. 419-425.

[4] O. Hod, "Graphite and hexagonal boron-nitride have the same interlayer distance. Why?", *J. Chem. Theory Comput.* **8** (2012), no. 4, p. 1360-1369.

[5] G. Cassabois, P. Valvin, B. Gil, "Hexagonal boron nitride is an indirect bandgap semiconductor", *Nat. Photonics* **10** (2016), no. 4, p. 262-266.

[6] J. D. Caldwell, I. Aharonovich, G. Cassabois, J. H. Edgar, B. Gil, D. N. Basov, "Photonics with hexagonal boron nitride", *Nat. Rev. Mater.* **4** (2019), no. 8, p. 552-567.

[7] B. Gil, G. Cassabois, R. Cusco, G. Fugallo, L. Artus, "Boron nitride for excitonics, nano photonics, and quantum technologies", *Nanophotonics* **9** (2020), no. 11, p. 3483-3504.

[8] R. Camphausen, L. Marini, S. A. Tawfik, T. T. Tran, M. J. Ford, S. Palomba, "Observation of near-infrared sub-Poissonian photon emission in hexagonal boron nitride at room temperature", *APL Photonics* **5** (2020), no. 7, article no. 076103.

[9] J. Koskelo, G. Fugallo, M. Hakala, M. Gatti, F. Sottile, P. Cudazzo, "Excitons in van der Waals materials: from monolayer to bulk hexagonal boron nitride", *Phys. Rev. B* **95** (2017), no. 3, article no. 035125.

[10] C. Elias, P. Valvin, T. Pelini, A. Summerfield, C. J. Mellor, T. S. Cheng, L. Eaves, C. T. Foxon, P. H. Beton, S. V. Novikov, B. Gil, G. Cassabois, "Direct band-gap crossover in epitaxial monolayer boron nitride", *Nat. Commun.* **10** (2019), no. 1, article no. 2639.

[11] P. Valvin, T. Pelini, G. Cassabois, A. Zobelli, J. Li, J. H. Edgar, B. Gil, "Deep ultraviolet hyperspectral cryomicroscopy in boron nitride: photoluminescence in crystals with an ultra-low defect density", *AIP Adv.* **10** (2020), no. 7, article no. 075025.

[12] L. Schué, L. Sponza, A. Plaud, H. Bensalah, K. Watanabe, T. Taniguchi, F. Ducastelle, A. Loiseau, J. Barjon, "Bright luminescence from indirect and strongly bound excitons in h-BN", *Phys. Rev. Lett.* **122** (2019), no. 6, article no. 067401.

[13] K. Watanabe, T. Taniguchi, H. Kanda, "Direct-bandgap properties and evidence for ultraviolet lasing of hexagonal boron nitride single crystal", *Nat. Mater.* **3** (2004), no. 6, p. 404-409.

[14] L. Wirtz, A. Marini, A. Rubio, "Excitons in boron nitride nanotubes: dimensionality effects", *Phys. Rev. Lett.* **96** (2006), no. 12, article no. 126104.

[15] F. Paleari, T. Galvani, H. Amara, F. Ducastelle, A. Molina-Sánchez, L. Wirtz, "Excitons in few-layer hexagonal boron nitride: Davydov splitting and surface localization", *2D Mater.* **5** (2018), no. 4, article no. 045017.

[16] C. M. Chow, H. Yu, A. M. Jones, J. R. Schaibley, M. Koehler, D. G. Mandrus, R. Merlin, W. Yao, X. Xu, "Phonon-assisted oscillatory exciton dynamics in monolayer $MoSe_2$", *NPJ 2D Mater. Appl.* **1** (2017), no. 1, article no. 33.

[17] T. Q. P. Vuong, G. Cassabois, P. Valvin, S. Liu, J. H. Edgar, B. Gil, "Exciton–phonon interaction in the strong-coupling regime in hexagonal boron nitride", *Phys. Rev. B* **95** (2017), no. 20, article no. 201202.

[18] T. Q. P. Vuong, S. Liu, A. Van der Lee, R. Cuscó, L. Artús, T. Michel, P. Valvin, J. H. Edgar, G. Cassabois, B. Gil, "Isotope engineering of van der Waals interactions in hexagonal boron nitride", *Nat. Mater.* **17** (2018), no. 2, p. 152-158.

[19] L. Schué, B. Berini, A. C. Betz, B. Plaçais, F. Ducastelle, J. Barjon, A. Loiseau, "Dimensionality effects on the luminescence properties of hBN", *Nanoscale* **8** (2016), p. 6986-6993.

[20] R. Ishii, M. Funato, Y. Kawakami, "Pushing the limits of deep-ultraviolet scanning near-field optical microscopy", *APL Photonics* **4** (2019), no. 7, article no. 070801.

[21] K. Watanabe, T. Taniguchi, "Far-UV photoluminescence microscope for impurity domain in hexagonal-boron-nitride single crystals by high-pressure, high-temperature synthesis", *NPJ 2D Mater. Appl.* **3** (2019), no. 1, p. 1-5.

[22] I. Stenger, L. Schué, M. Boukhicha, B. Berini, B. Plaçais, A. Loiseau, J. Barjon, "Low frequency Raman spectroscopy of few-atomic-layer thick hBN crystals", *2D Mater.* **4** (2017), no. 3, article no. 031003.

[23] J. Zribi, L. Khalil, J. Avila, J. Chaste, H. Henck, F. Oehler, B. Gil, S. Liu *et al.*, "Structural and electronic transitions in few layers of isotopically pure hexagonal boron nitride", *Phys. Rev. B* **102** (2020), no. 11, article no. 115141.

[24] K. Luo, X. Yuan, Z. Zhao, D. Yu, B. Xu, Z. Liu, Y. Tian, G. Gao, J. He, "New hexagonal boron nitride polytypes with triple-layer periodicity", *J. Appl. Phys.* **121** (2017), no. 16, article no. 165102.

[25] H. Henck, D. Pierucci, Z. B. Aziza, M. G. Silly, B. Gil, F. Sirotti, G. Cassabois, A. Ouerghi, "Stacking fault and defects in single domain multilayered hexagonal boron nitride", *Appl. Phys. Lett.* **110** (2017), no. 2, article no. 023101.

[26] L. Sponza, H. Amara, C. Attaccalite, S. Latil, T. Galvani, F. Paleari, L. Wirtz, F. Ducastelle, "Direct and indirect excitons in boron nitride polymorphs: A story of atomic configuration and electronic correlation", *Phys. Rev. B* **98** (2018), no. 12, article no. 125206.

[27] S. Matt Gilbert, T. Pham, M. Dogan, S. Oh, B. Shevitski, G. Schumm, S. Liu, P. Ercius, S. Aloni, M. L. Cohen, A. Zettl, "Alternative stacking sequences in hexagonal boron nitride", *2D Mater.* **6** (2019), no. 2, article no. 021006.

[28] L. Xian, D. M. Kennes, N. Tancogne-Dejean, M. Altarelli, A. Rubio, "Multiflat bands and strong correlations in twisted bilayer boron nitride: doping-induced correlated insulator and superconductor", *Nano Lett.* **19** (2019), no. 8, p. 4934-4940.

[29] X.-J. Zhao, Y. Yang, D.-B. Zhang, S.-H. Wei, "Formation of bloch flat bands in polar twisted bilayers without magic angles", *Phys. Rev. Lett.* **124** (2020), no. 8, article no. 086401.

[30] H. Ochoa, A. Asenjo-Garcia, "Flat bands and chiral optical response of Moiré insulators", *Phys. Rev. Lett.* **125** (2020), no. 3, article no. 037402.